(28) Wallington, T. J.; Skewes, L. M.; Siegl, W. O.; Wu, C.-H.; Japar, S. M. *Int. J. Chem. Kinet.* **1988**, *20*, 867.
(29) Wine, P. H.; Semmes, D. H. *J. Phys. Chem.* **1983**, *87*, 3572.
(30) Heneghan, S. P.; Knoot, P. A.; Benson, S. W. *Int. J. Chem. Kinet.* **1981**, *13*, 677.
(31) Lewis, R. S.; Sander, S. P.; Wagner, S.; Watson, R. T. *J. Phys. Chem.* **1980**, *84*, 2009.
(32) Tschuikow-Roux, E.; Yano, E.; Niedzielski, J. *J. Chem. Phys.* **1985**, *82*, 65.
(33) Tschuikow-Roux, E.; Faraji, F.; Paddison, S.; Niedzielski, J.; Miyokawa, K. *J. Phys. Chem.* **1988**, *92*, 1488.
(34) Atkinson, R.; Baulch, D. L.; Cox, R. A.; Hampson, R. F., Jr.; Kerr, J. A.; Troe, J. *Atmos. Environ.* **1992**, *26A*, 1187.
(35) Atkinson, R.; Aschmann, S. M. *Int. J. Chem. Kinet.* **1985**, *17*, 33.
(36) Tuazon, E. C.; Atkinson, R.; Corchnoy, S. B. *Int. J. Chem. Kinet.* **1992**, *24*, 639.
(37) Zahniser, M. S.; Berquist, B. M.; Kaufman, F. *Int. J. Chem. Kinet.* **1978**, *10*, 15.
(38) Atkinson, R. *Int. J. Chem. Kinet.* **1987**, *19*, 799.
(39) Atkinson, R. *Chem. Rev.* **1986**, *86*, 69.
(40) Laidler, K. J. *Chemical Kinetics*; Harper and Row: New York, 1987.
(41) Senkan, S. M.; Gutman, D. In *Combustion Chemistry*; Gardiner, W. C., Jr., Ed., in press.
(42) Cohen, N.; Westberg, K. R. *J. Phys. Chem. Ref. Data* **1992**, *20*, 1211.
(43) Senkan, S. M. *Adv. Chem. Eng.* **1992**, *18*, 95.
(44) Warnatz, J. In *Combustion Chemistry*; Gardiner, W. C., Jr., Ed.; Springer-Verlag: New York, 1984.

Temperature Dependence of Light Scattering from Neat Benzene with Femtosecond Pulses: Are We Seeing Molecules Librate?

Amir Waldman, Uri Banin, Eran Rabani, and Sanford Ruhman*

Department of Physical Chemistry and the Farkas Center for Light-Induced Processes, Hebrew University, Givat Ram, Jerusalem 91904, Israel *(Received: June 23, 1992; In Final Form: September 2, 1992)*

We report femtosecond impulsive stimulated scattering experiments on neat liquid benzene at 280 and 343 K. The results are compared with those of Litovitz and co-workers using dynamic light-scattering spectroscopy and found to agree quantitatively. In spite of the evidence for interaction-induced scattering intensities detected at early times, we analyze our results in terms of reorientation of single molecules in the liquid and determine that at temperatures below 310 K, we observe evidence of oscillatory angular velocity correlation functions (AVCF's). These oscillations become more pronounced as the liquid is cooled further, and the time evolution of the correlation indicates that librational motion is predominantly dephased by inhomogeneous mechanisms. We discuss the ubiquitous nature of this finding in many molecular liquids near the crystallization temperature and stress the importance of investigating the fact that MD simulation studies have not generated AVCF's that resemble damped harmonic oscillations, with multiple crossings of the origin, in this thermodynamic regime.

I. Introduction

Molecular motions in liquids have been extensively probed through the application of light-scattering spectroscopy.[1-3] Gordon's classic papers highlight the role of reorientation on the form of the spectral lines.[4] Further scrutiny, however, including work in the gas phase, revealed the substantial contribution of interaction-induced (II) polarizability components to the observed dynamical light-scattering spectral (DLSS) line shapes.[5-8] The inseparability of the reorientational single-particle contributions from the II and collective light-scattering components renders the inference of specific reorientational dynamics of liquid particles from DLSS data ambiguous.

In spite of this, some general conclusions arise from analysis of Rayleigh and Raman scattering spectra for molecules of anisotropic structure and polarizability in the liquid phase. By disregarding contributions other than single-particle reorientations to the spectral broadening, one can derive approximate angular position and angular velocity autocorrelation functions (APCF's and AVCF's) from DLSS data.[1-4,9] The derived correlation functions qualitatively agree and, in specific cases, seem to render quantitative agreement with our intuitive understanding of the nature of reorientational motion in equilibrium molecular liquids. This motion begins with a stage of inertial "free" rotation followed by subsequent collisions with the surrounding molecules, which tend to revert the angular velocity and ultimately leads to relaxational decay of the angular position correlation following the complete dissipation of the angular velocity correlation.

In a number of highly anisotropic molecular liquids, near the freezing temperature, such analysis of the DLSS data leads to experimental AVCF's which exhibit clearly underdamped orientational oscillation and multiple reversals of sign.[10-12] Such observations are reported for carbon disulfide, methyl iodide, and benzene. In order to better understand the mechanisms giving rise to the scattering spectra, molecular dynamics (MD) calculations of these liquids have been undertaken, employing interparticular potentials which reproduce the thermodynamics of the liquids well.[13-15] The "cage"-induced reversal of angular momentum, which is the essence of librational reorientation in liquids, shows up as an intense negative portion of the simulated AVCF's prior to their decay to zero. Nonetheless, MD simulations of said liquids near freezing have not produced such ensemble-averaged measures of reorientation which exhibit multiple periodic reversals of sign. In cases where an effort has been made to make use of the MD results to simulate light-scattering spectra, even inclusion of II polarizability fluctuations in the simulations has not produced line shapes from which oscillatory AVCF's would be extracted.[16]

In recent years, the study of molecular motions in liquids has been reexamined through time-domain light-scattering techniques, mainly with femtosecond laser pulses[17-21] but also with incoherent laser radiation.[22] In the various implementations of impulsive stimulated light scattering (ISS), including impulsive optical Kerr effect experiments,[19b] the motions which modulate the dielectric constant and give rise to the DLSS are stimulated by "sudden" excitation of the liquid by intense ultrashort laser pulses. The evolution of the stimulated motions is followed by probing the induced anisotropy of the liquid by a delayed weak probe pulse of similar duration. The extensive activity in this field is motivated not only by our fascination with the ability to manipulate elementary molecular motions in real time but also by the well-founded anticipation that due to the Fourier transform relation between the time and frequency domain data, the early inertial motions which show up in the DLSS as low-intensity wings will be more prominent and more accurately characterized through the ISS results.[23]

This promise has not yet been fully realized for two main reasons. In numerous applications of this technique, the existence of an instantaneous electronic dielectric response has masked the first portion of the nuclear response—precisely that portion which

0022-3654/92/2096-10842$03.00/0

it was deemed best suited to recover. But as was elegantly demonstrated by Etchepare et al., implementing the ISS experiment in a box geometry with proper control of the polarization of all four waves involved can eliminate the electronic contribution.[24] Even so, the fact that most groups have employed pulses a few tens of femtoseconds in duration requires deconvolution to reveal the dynamical response at times shorter than the pulse cross-correlations! This is a demanding proposition and requires outstanding signal-to-noise both in ISS data and in measurements of the pump and probe cross-correlation.

The gross relaxation times derived from ISS results on molecular liquids to date have in general agreed with those from frequency-domain work. The problem of separating out II-scattering components has eluded experimenters with ISS, and probing its existence and its relative magnitude in the ISS response are central issues of discussion. In accordance with DLSS results, cryogenically cooled CS_2 develops an extra weak shoulder in the ISS response,[19,25] and AVCF's derived from such data using Kubo line-shape theory have been shown by Ruhman and Nelson to develop underdamped dynamics near the freezing point. Kohler and Nelson have shown similar behavior for room-temperature CS_2 at a few kilobars of pressure.[26] In both cases, these results have been interpreted to indicate true underdamped librational motions of the monomers. Numerous reports have also demonstrated ISS data of similar appearance for neat benzene at room temperature.[19b-22,27] Analogous results for pressurized CS_2 have been obtained using DLSS; however, the promoted interpretation was somewhat different.[38] Specific efforts to reproduce recurrent time-domain dielectric responses using elaborate MD simulations have been unsuccessful.[39]

In the following report, we present new ISS results on neat benzene in the temperature range of 7–70 °C. This study aims to make a critical comparison of the dynamical information obtained through ISS with that previously extracted from DLSS data.[28] Benzene is an ideal candidate for this purpose due to the elaborate experiments by Litovitz and co-workers especially in view of the approach chosen by those authors for analysis (hereafter this reference will be designated as paper I). Through this, a better appreciation of the inherent limitations of either technique will emerge. In addition, we will demonstrate the large similarity of ISS signal variations upon cooling of neat benzene and carbon disulfide near their freezing points. Accordingly, we will argue that it is most likely that these changes are due mainly to variations in the reorientational motions of single molecules in the liquids and transition to oscillatory AVCF's. Through the presented results, we stress the generality of experimentally derived underdamped AVCF's and underline the importance of clearing up the discrepancy between experiment and theory concerning this issue.

The organization of the paper is as follows: this introduction will be followed by a short summary of the essential theoretical background in section II. Following that, we will give a full description of our recently constructed experimental setup and relevant technique in section III. In section IV, we will first summarize our results, including analysis, careful deconvolution of the data, and extraction of experimental AVCF's. Section V will be dedicated to comparing these results with those obtained by DLSS, and section VI is a general discussion and conclusion.

II. Theoretical Background

The ISS experiment has been theoretically described in detail elsewhere[29] and the approach used here for analysis outlined in a recent publication.[25] We will therefore only summarize the most important results for a clear presentation of the procedure followed here in our data reduction.

$S(t)$, the signal which is measured in the ISS experiment, may be given in terms of the relevant projection of the dielectric response tensor, $G^{\epsilon\epsilon}(t)$, as follows:

$$S(t) = \int_{-\infty}^{+\infty} \left| \int_{-\infty}^{t'} G^{\epsilon\epsilon}(t' - t'') I^{E}(t'')\, dt'' \right|^2 I^{P}(t' - t)\, dt' \quad (1)$$

where the temporal envelopes of the excitation and probing pulses are designated I^E and I^P, respectively, and t' and t'' are two dummy time arguments which are necessary for implementation of the proper convolutions. Bold italic symbols are reserved throughout for tensors and tensor functions only. The tensor $G^{\epsilon\epsilon}$ describes a third-order nonlinear response and is therefore of fourth order. In order to define the experiment fully, one must define four polarization directions for the light waves involved in the process—two excitation fields, one probe, and one scattered wave. In the limit of pump and probe pulses of negligible duration, this double integral reduces to the simple form

$$S(t) = |G^{\epsilon\epsilon}(t)|^2 \quad (2)$$

Disregarding the task of deconvolution for the time being, through the ISS experiment, we therefore have direct access to the absolute value of the dielectric response. In the high-temperature limit, the autocorrelation function of the dielectric constant (again a fourth-order tensor which is a function of time) can be derived by the relation

$$C^{\epsilon\epsilon}(t) \propto -\left(\int_t^{\infty} G^{\epsilon\epsilon}(t')\, dt' \right) \quad (3)$$

This autocorrelation function is obtained from DLSS data through Fourier transformation of the Boltzmann weighted line-shape function[1-4] and is the meeting ground for the comparison of dynamical information collected by both of these complementary techniques.

The origins of interaction-induced variations in molecular polarizabilities and the mechanisms by which these variations influence the time evolution of $C^{\epsilon\epsilon}$ in condensed systems have been discussed in detail by many authors and are the subject of ongoing study and debate. We will not attempt to cover this issue here. Remembering that $C^{\epsilon\epsilon}$ has the dimensions of polarizability squared, we can project out the reorientational contribution schematically by the following division:

$$C^{\epsilon\epsilon}(t) = C^{OR}(t) + C^{II}(t) + C^{CT}(t) \quad (4)$$

where $C^{CT}(t)$ represents the cross terms involving time correlations of II variations in polarizabilities, with orientational ones at previous or later times. We also neglect any correlations between reorientation and translational motions of the monomers. It should be stressed at this point that if translational motions alone were capable of generating the recurrent dielectric responses observed near the freezing point, then we could expect these results not only in molecular liquids of highly anisotropic monomers. If we disregard both the II and CT terms and further disregard pair correlations in $C^{OR}(t)$, we are left with an approximate correlation function due to single-molecule polarization anisotropies, $C_2'(t)$, which is now simply the single-molecule APCF relevant to χ^3 nonlinear spectroscopies for symmetric top symmetry:

$$C^{OR}(t) \cong C_2'(t) \equiv \tfrac{3}{2}\langle \cos^2(\theta(t)) - \tfrac{1}{3} \rangle \quad (5)$$

The 2 subscript indicates we are following the correlation in time of a second-order tensor ϵ, and θ is the spherical angle between the direction in space of the molecular symmetry axis at time zero and time t. The angular brackets indicate ensemble averaging. The near equality between $C_2'(t)$ and $C^{OR}(t)$ at long time delays, in the case of liquid benzene, has been demonstrated experimentally as discussed by Dardy et al. in paper I and will be elaborated further in section V.

While in $C_2'(t)$ we have finally reduced our scope to single-molecule characteristics, the APCF in the most general sense must be derived by integration of a stochastic differential equation involving the AVCF, as described by Kubo for a generalized ensemble of oscillators in condensed media[30] and applied to the problem of reorientation in solution.[9,31,32] Referring the interested reader to the cited literature for details, we limit ourselves here to the result of that analysis for symmetric top monomers, giving the normalized AVCF from the APCF according to

$$C_\omega(t) = -(I/6kT) \frac{d^2}{dt^2} \ln [C_2'(t)] \quad (6)$$

I is the moment of inertia for rotation of the symmetry axis and k is Boltzmann's constant. $C_\omega(t)$, the normalized AVCF, allows characterization of the average reorientational dynamics of single monomers in a thermal ensemble of molecules.

Before concluding this section, we comment on the relationship, defined in 6, between the APCF and the AVCF. If, indeed, the initial value of the AVCF is one, it can be shown readily that, at least for early times, $\ln[C_2'(t)] = -(3kT/I)t^2$, precisely the behavior of an ensemble of free rotors of inertia I and temperature T. At longer times, after all the correlation of angular velocity has died out, it can similarly be shown that eq 6 predicts a linear decay of the natural logarithm of the APCF with a slope of $-(6kT/I)\tau_c$, where τ_c is the angular velocity correlation time and is derived by a time integral from $t = 0$ to infinity of the normalized AVCF. Finally, it should be stressed again that through the ISS experiments, we have no direct access to $C_2'(t)$ but rather to $C^{ee}(t)$ and in our analysis will be replacing it for the former. Therefore, the compliance of the approximate AVCF derived by applying eq 6 to $C^{ee}(t)$, with the discussed limiting behaviors at early and long times, may be used as a criterion for estimating the dominance of single-molecule reorientation relative to II mechanisms, in generating the dielectric response in neat benzene.

III. Experimental Section

The laser system constructed for these experiments is similar to others reported in the literature,[19,33] and we will emphasize the novel aspects of this one and describe the details concerning the experimental configuration. Our source of femtosecond pulses is an antiresonant ring synch-pumped dye laser constructed in lab and operating at 82 MHz with the rhodamine 6G/DODCI dye pair. The reflectors surrounding the rhodamine jet and the DODCI jet are of 10- and 5-cm radii of curvature, respectively. The gain dye jet is commercial (Coherent) and that for the saturable absorber homemade with a path length of 10–20 μm. The laser was run with four Brewster prisms, with no spectral aperturing.

The dye laser is pumped with the frequency-doubled output of an acousto-optically mode-locked (AOML) and power-stabilized (±1%) Nd:YLF laser (Quantronix 417) for which we supplied a custom-made rf source as part of an active stabilization scheme for the dye cavity. Synch-pumped femtosecond dye lasers are known to be so stringently dependent upon cavity length that in most cases active stabilization is required for long- and short-term stability of operation.[34,35] We have chosen to achieve this by combining the control of the cavity length via a piezoelectric actuator for correcting low-frequency "drift", with slight variations of the rf frequency going to the mode locker for correcting effective cavity length fluctuations at high frequencies.

The correction signal was generated by dispersing the beam transmitted through a cavity high reflector onto a single PIN photodiode. The difference between the current signal from the photodiode and an adjustable dc current source generated a correctional signal which was passed through high- and low-pass filters before being fed into the voltage-controlled frequency generator for the mode locker (Vectron) and into the high-voltage amplifier and piezoelectric positioner, respectively. In this configuration, the piezoelectric actuator corrected for perturbations at frequencies from dc up to nearly 1 Hz and the rf modulation corrected perturbations from 1 to 200 Hz. The slight variations in the rf frequency required to stabilize the dye laser (±10 Hz) had no detrimental effects on the YLF laser operation. The typical output of the stabilized dye laser is pulses containing 0.4 nJ of energy with a duration of 60 fs and a central frequency of 615 nm, which due to the active stabilization could be operated continuously for hours without recourse to pneumatical isolation of the optical platform.

The dye laser pulses were amplified in a synchronous three-stage dye amplifier which was pumped by the doubled output of a Nd:YLF regenerative amplifier (RA). The RA was constructed around a commercial CW YLF cavity (Quantronix, 117) prepared for operation as a RA for a AOML laser operating at 76 MHz. After adjustment of the cavity length for operation at 82 MHz, acousto-optic (Newport Electro Optics) and electro-optic (Laser Metrics) modulators were added to the amplifier. The electro-optic modulator was configured as a Pockel's cell, using a homemade avalanche transistor driver. The single-pulse selection and seeding of the RA were performed as previously described.[33] The maximum output of the RA was 3.5 mJ pulses at a repetition rate of 1 kHz and with a peak-to-peak stability of 2–3%. The duration of these light pulses was not directly measured but is expected to be similar to that of the seed pulses—70–100 ps. In our experiments, the output was limited to 1.1 mJ/pulse and frequency doubled with an efficiency of ~50% in KTP.

These green pulses were combined collinearly with the dye laser pulses in three amplification stages containing sulfarhodamine 640 in water and ethanol, producing amplified pulses with an average energy of 30 μJ/pulse, at the repetition rate of 1 kHz. After compensation for group velocity dispersion in a prism pair, the duration of these pulses was identical to that prior to the amplification. Beam splitting, white-light continuum generation, focusing on the sample, and signal processing were performed according to the method described previously.[25,33] Benzene liquid (Aldrich, spectrograde) was sealed by flame in a 2-mm cell after a few freeze–thaw cycles, and the temperature of the sample was controlled by pressing the cell onto a brass holder through which water from a constant-temperature water bath was circulated. The temperature of the sample was determined with an estimated accuracy of ±1 K, and the pressure of the samples was the vapor pressure of the benzene liquid.

The configuration of polarizations chosen for pump probe and signal waves, in order to eliminate electronic contributions to the ISS signal, was a variant of the one previously described by Ruhman and Nelson.[25] The two pump beams are both polarized parallel to the wavevector of the interference grating they create, and we define this direction as our origin (0°). The probe polarization was directed at an angle of +60° to the direction of the pump polarizations, and the signal was viewed through a polarizer transmitting radiation at an angle of −60°. This configuration was employed both for the experiments where all three input beams were directly derived from laser pulses at 615 nm and for the experiments where the probe beam was derived from a white-light continuum portion at 640 nm. It was preferred over the configuration previously used on cooled CS_2, since it allows preparation of both pump beams in the same polarization. The intensity of the exciting pulses was systematically reduced until the time evolution of the signal was unchanged by further reduction. For purposes of signal deconvolution, an autocorrelation scan of the amplified pulses was collected before each set of experiments. During the experiments, a reorientation of the signal-viewing polarizer allowed the recording of the instantaneous electronic ISS response in a slide of fused silica, and this signal was used to determine a third-order cross-correlation for experiments using continuum pulses for probing and a third-order autocorrelation for the fundamental amplified pulses.

IV. Results

ISS data were collected at a number of temperatures within the range of 7–70 °C. Experiments conducted with white-light probe pulses and with fundamental laser probe pulses showed identical time dependencies. Due to the limited range of temperatures tested and the gradual nature of signal variation within this range, we have limited our analysis to the data obtained at the lowest and highest temperatures only. In Figure 1, we present a linear and a log plot of the raw data at these extreme temperatures. The near absence of the immediate electronic response at $t = 0$ is apparent. The remaining nuclear response is in every way qualitatively similar to the response reported for cold carbon disulfide. At 70 °C, the signal consists of a rapid rise which reaches a maximum at a delay of ~120 fs between pump and probe pulses—clearly after the stage of excitation is over. The signal then decays rapidly down to nearly 10% of its peak value within another 200 fs, then giving way to a much slower nearly exponentially relaxing stage with an average decay time of ~0.6 ps. With the pulse duration employed here, a very weak second

TABLE I: Parameters of the Best Fit to Data

T, K	Δ, fs^{-1}	ω, rad/fs	A	γ_a, fs^{-1}	Γ_a, fs^{-1}	B	γ_b, fs^{-1}	Γ_b, fs^{-1}	C	γ_c, fs^{-1}
280	0.006 26	0.0126	8.61	0.006 65	0.007 24	0.205	0.000 41	0.006 86	7.49	0.006 66
343	0.006 99	0.0109	2.626	0.006 08	0.007 62	0.285	0.000 77	0.006 74	−1.5	0.007 43

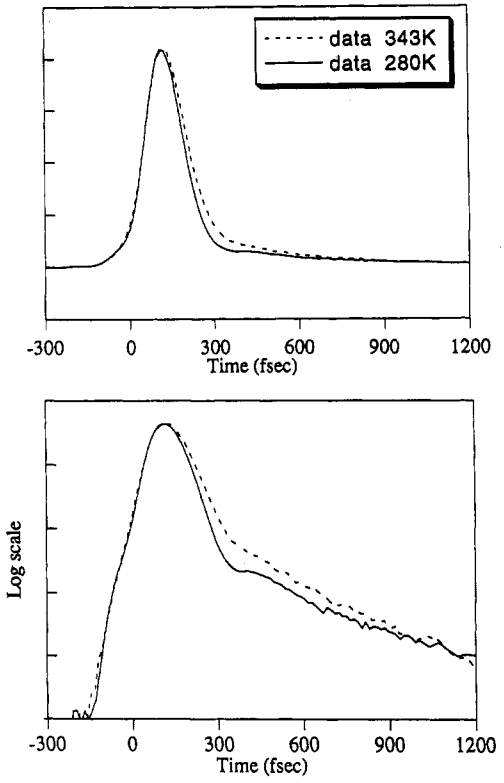

Figure 1. ISS signals obtained for neat benzene at 280 and 343 K presented as a function of pump and probe delay on a linear and logarithmic scale.

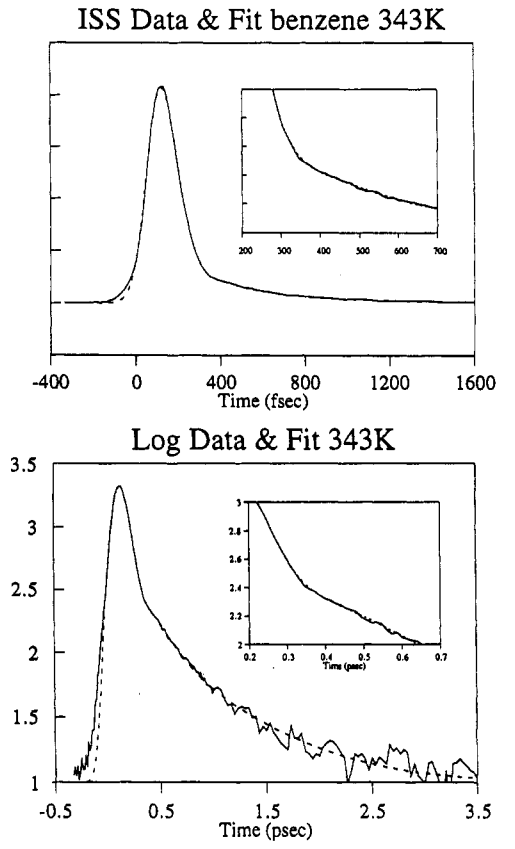

Figure 2. Experimental ISS signal at 343 K presented as a continuous line along with the best fit rendered by eq 7 depicted with a dashed curve. The log plot demonstrates the ability of this functional form to reproduce the data over more than 2 decades of decay. The parameters used for these fits are presented in Table I.

shoulder or recurrence following the rapid initial decay of the signal can only barely be observed. Upon cooling to 7 °C, the signal is observed to decay even more rapidly following the initial rise, falling fully to 7% of the peak intensity, but then demonstrating a clear recurrence of signal and giving way to a slow decay which is more pronouncedly nonexponential. The shoulder eluded to is most clearly demonstrated in the log plot of the data.

The employed procedure of data deconvolution from the influence of the finite width of our laser pulses was as follows. The data were fit to a multiparameter test function for the dielectric response $G^{\epsilon}(t)$ after they had first been numerically convoluted with the experimentally derived temporal profiles of our laser pulses and squared according to eq 1. The optimization was performed using a Marquardt–Levenberg least-squares routine.[36] The approximate profiles of our pulses were derived by first fitting nonlinear autocorrelation traces with a test function that was a linear combination of a Gaussian and a hyperbolic secant squared. In all cases, the Gaussian component required for the best fit contributed less than 10% of the intensity at zero time. Later these profiles were further tested by using them to reconstruct a third-order autocorrelation function and comparing them with the results derived from electronic ISS responses.

The functional form used for the dielectric response is the same as that used previously for ISS data for carbon disulfide:[25]

$$G^{\epsilon}(t) \propto e^{-\Delta^2 t^2/2} \sin(\omega t) + A(e^{-\gamma_a t} - e^{-\Gamma_a t}) + B(e^{-\gamma_b t} - e^{-\Gamma_b t}) + C(e^{-\gamma_c t} - e^{-\Gamma_b t}) \quad (7)$$

The least-squares fitting serves to deconvolute the data from our experimental machine response and to prepare our results for further theoretical analysis. Presentation of Green's function in an analytical parametrized form also allows others to reconstruct our data independently. The quality of the fit rendered by the procedure we have described is demonstrated in Figure 2, where we show both the data and the results of the best fit for one temperature on linear and log scales. The parameters used to obtain these fits are presented in Table I. A small discrepancy between all trial functions used and our data is found for times ± 40 fs and is suspected to be due to residual electronic responses due to slight depolarizations of our probing beam from thermal strain in the cells. Even so, the relative intensity of the electronic response has been lowered by more than 2 orders of magnitude.

After generating the analytical Green functions of the dielectric constant at both temperatures, the time autocorrelation function $C^{\epsilon}(t)$ is derived by integration with respect to delay time according to eq 3 and normalization to the value at $t = 0$. As described in section II, we will hereafter use this correlation function as an experimental measure for $C_2'(t)$ and designate it as an APCF. In doing so, we are not in any way making a statement concerning the importance of including II effects in light-scattering data. This course of action mirrors our inability at this stage to extract $C_2'(t)$ directly and our doubts concerning procedures which subtract approximate estimates of $C^{II}(t) + C^{CT}(t)$.

The results are depicted in Figure 3, showing the experimentally derived APCF's at 280 and 343 K along with the expected limiting behavior of thermal free rotors as a function of reduced time, $t^* = t(kT/I)^{1/2}$. Qualitatively, these correlation functions are similar to those extracted from both ISS for other systems and for benzene from DLSS data.[1-4,10-12,28] They show an early stage of parabolic decay followed by a slowing down of the relaxation and a transition to what appears to be a nearly exponential decay. At the lower temperature, the transition happens earlier on, and a very weak

TABLE II: Parameters of the Fit to the Experimental AVCF

T, K	A	B	ω, rad/fs	Θ, fs^{-1}	α, fs^{-1}	β, fs^{-1}
280	1.29	1.027	0.016	0.26	0.001 37	0.0059
343	1.238	1.026	0.015	0.24	0.001 49	0.0063

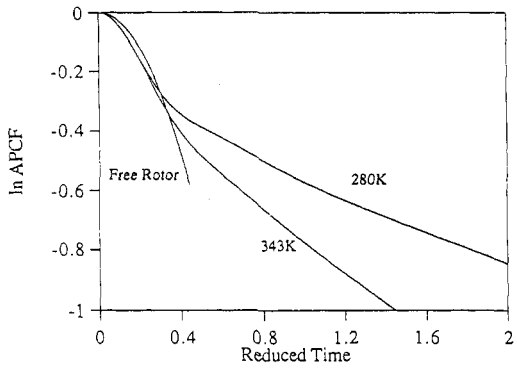

Figure 3. Experimentally derived angular position correlation functions for both temperatures presented on a ln scale along with the limiting short-time behavior for thermal free rotors. All curves are depicted against a reduced time variable. The considerable discrepancies at early times are clearly discernible.

shoulder is apparent at the onset of this change. Already at this stage we can see substantial differences between the behavior of the experimental APCF and free rotor decay of orientation at early times. The experimental correlation functions decay more rapidly than the predictions for free rotors.

This difference becomes much more striking when AVCF's are extracted from the derived APCF's according to eq 6, as depicted in Figure 4. The initial value of exact single-molecule-normalized AVCF's is equal to unity.[1-4] Our experimental approximations of AVCF's exceed this value almost by a factor of 2. The initial values that we obtain at 280 and 343 K are 1.8 and 1.65, respectively. The estimated error to be associated with these values is ±10%. At both temperatures, the AVCF traverses zero three times; however, the oscillatory nature is much more manifest at 280 K, and the low-amplitude-persistent negative portion of the AVCF at 280 K is stronger. This phase of the AVCF indicates the nonexponential long-time decay of $C^{(2)}(t)$. Along with the AVCF's, we have also plotted the best fits to these functions using a test function of the form

$$C_\omega(t) = A\left[\left(B\cos(\omega t) + (2\alpha - \Theta)\left(\frac{1-A}{\omega}\right)\sin(\omega t)\right)\times \exp(-\beta^2 t^2/2) + (1-B)(2\exp(-\alpha t) - \exp(-\Theta t))\right] \quad (8)$$

This functional form is nearly that of a Gaussian distribution of oscillator frequencies. The consequences of β being nearly as large as ω have been discussed in detail in ref 25. Aside from the initial 50 fs, eq 8 is capable of reproducing the AVCF's extremely well. Functional forms based on exponentially decaying harmonic oscillations were not capable of rendering a reasonable fit to these correlation functions even when the first 100 fs of the AVCF's was ignored for purposes of summing squares. The parameters used to obtain the best fits are listed in Table II.

V. Discussion

We will dedicate our discussion to three main issues: first to the question of accuracy with which we have recorded the dielectric response using ISS, including a comparison of our results with those of Dardy et al.;[28] second whether we may learn fine details of molecular reorientational dynamics from this data; finally the implications of the consistent discrepancies between the interpretation we propose for our results and published studies using MD calculations concerning reorientational dynamics of single molecules in model liquids.

The only means we have to estimate the accuracy of our deconvolution method is obtained from the comparison of the temporal profiles of our pulses derived from nonlinear intensity autocorrelation traces and purely electronic ISS data. In all cases studied, we have obtained profiles that agree to within 5% in the duration FWHM and find very similar functional forms. We are therefore confident that we have obtained a good approximation for the pulse intensity profiles.

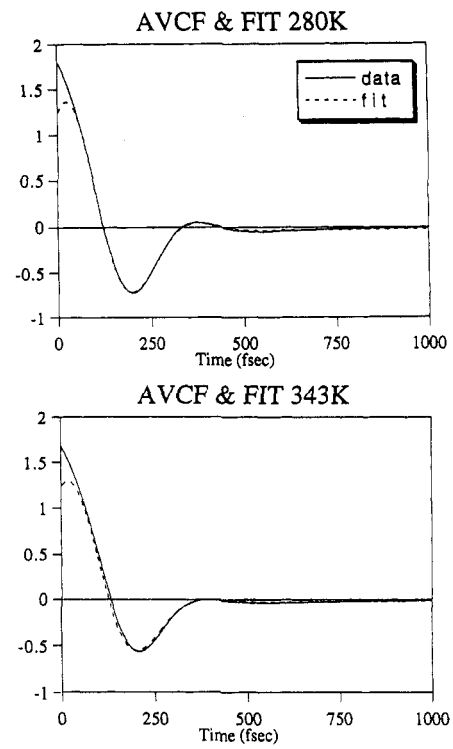

Figure 4. Experimentally derived AVCF's presented (full curve) along with the best fit rendered by application of eq 8. Parameters for these fits are presented in Table II.

Beyond the considerations of our procedure for eliminating machine response effects, we may look for qualitative agreement of our results with ISS experiments in other liquids, but for quantitative assessments, we must rely on comparison with DLSS work on the identical system. This approach is problematic since to begin with we anticipated that ISS might be a more reliable and clearly more direct experimental method for obtaining the time dependence of the dielectric response at early times. We are fortunate that Litovitz and co-workers obtained DLSS with outstanding signal-to-noise ratios and that the initial curvature of the obtained $C^{(2)}(t)$ was a central issue of discussion in their work.

We will begin by comparing our results for the behavior of the autocorrelation function of the dielectric constant near $t = 0$. The curvature referred to gives the initial values of our experimental AVCF and can be obtained directly from the DLSS data as the ratio of the second to the zeroth spectral moments. For free rotors devoid of pair correlations, the expected value for $C_\omega(0) = 1$. The initial values of our AVCF's exceed this value by factors of 1.8 and 1.65 (±10%) for 280 and 343 K, respectively. Dardy et al. report for similar temperatures excesses of 2.15 and 1.86. If we assume a similar uncertainty in these numbers, we find not only an agreement in the existence of such an excess and its variation with temperature *but also a quantitative agreement of the magnitude of these excesses within expected bounds of error*!

At intermediate delay times, it is difficult to make a quantitative comparison with the DLSS results since they are presented as AVCF's following a subtraction of an II correlation component. As we will discuss later, we have not used this method and therefore can only test the qualitative agreement of the experi-

mental AVCF's obtained by both methods. In many respects, they agree remarkably. At the lowest temperatures, the derived AVCF's traverse zero three times, giving way to persistent negative values after ~350 fs. At the highest temperatures (343–350 K), this trend has just been erased, with a lesser extent of long-term negative portion. The relative magnitudes of the positive and long-term negative portions are also in agreement.

Finally, at long delay times, $C^{(2)}(t)$ decays nearly exponentially, mirroring a relaxational angular diffusion, and we can compare the mean relaxation times derived from the DLSS and ISS results. Dardy et al. did not reduce the temperature of benzene below 286 K, but the asymptotic decay time which is referred to in their paper as τ_{OR} may be inferred from the linear plot in Figure 11 of paper I. Ironically, perhaps the portion of the dielectric response where our results disagree most markedly with those presented in paper I in this long-term decay. We find that the $C^{(2)}(t)$ values we derive are much more nearly exponential and on a log scale appear essentially linear after a picosecond of delay. While the asymptotic slopes we recover for the higher temperatures agree with those of Dardy et al. (0.77 and 0.73 ps^{-1}, respectively), the long-term decay at low temperatures is substantially different. It is tempting to associate these discrepancies with the subtraction of the II portion of the correlation function; however, at long times, this subtraction should have little effect on the time dependence of the correlation decay. Understanding this point may require closer scrutiny of the frequency-domain results. It is interesting to note that the required relation of the rate of decay for angular position at long times and the τ_c calculated from the APCF of paper I does not fulfill the relation required in the line-shape theory and presented in section II.

To summarize this portion of the discussion, as a whole, the agreement of our results with those of Dardy et al. is extremely good, especially at early times. This is the most convincing demonstration to date of the equivalence of these approaches for studying dielectric response with high time resolution. By saying this, however, we must also agree that at least for the case of benzene, either approach is sufficient for abstracting reliable dielectric response dynamics.

In view of this similarity, our interpretation must address the same basic issues discussed in paper I and in the works of Nelson and co-workers.[25,26] The excess in the initial value of our experimental AVCF clearly indicates that during the first tens of femtoseconds, II polarizabilities are contributing to our ISS signals. A similar result was obtained for cooled carbon disulfide, but insufficient knowledge of the pulse shapes used left large uncertainties concerning this point.[25] Both the time scale involved and the observation provided by Dardy et al. concerning the similarity of reorientational relaxation times derived from NMR, Raman, and Rayleigh spectral line shapes exclude the complicity of pair correlations in this discrepancy. The quantitative agreement between the DLSS and ISS results in this respect shows beyond doubt the authenticity of this effect. In paper I, Litovitz and co-workers chose to extract a better approximation for $C_2'(t)$ by subtracting an estimated II contribution from the dielectric correlation function until free rotor behavior at early times is recovered. We feel uncomfortable with this procedure since we have no way of independently testing the relevance of the temporal form assumed for the II contribution in this specific case.

The main question we must answer is whether we can extract information concerning single-molecule reorientations at all delay times, despite the clearly observable presence of II contributions to our signal. In view of the expected time scales for II contributions[28] and the stated absence of pair correlation effects, we propose that our data at times beyond 100–150 fs reliably mirror the behavior of the AVCF. Thus, our *quantitative* time-domain corroboration of the benzene work in paper I, the pressure and temperature experiments with CS_2 both in the time and frequency domains, and additional work on other systems build a conclusive case that in fact cooling induces a transition to oscillatory AVCF's. Since this is an ensemble-averaged function, this transition requires not only that on average single molecules librate beyond one period in this and in other molecular liquids of strongly anisotropic geometry and at temperatures that bring the liquid on the verge of crystallization, but also that the dynamics of libration are similar enough that the monomers will not lose step with each other within a single librational period. It seems very reasonable that near freezing, the structure of the liquid will become homogeneous enough and, due to the increased density, the restoring force to reorientation strong enough for the angular motions to undergo multiple changes in sign before dephasing. Our proposition concerning interpretation of our data is not original, but our results provide yet another confirmation of the generality of the observed phenomenon, this time directly in the time domain.

The fact that only Gaussian decay models of the AVCF's were capable of fitting the data even after ignoring the first 100 fs of delays indicates further that inhomogeneity of the liquid and of the frequencies of libration is a major factor in the dephasing of libration in molecular liquids.[25,32] It is important to state that the initial divergence of the best fit of eq 8 and experimental AVCF's is just what we expect given the existence of rapidly decaying II scattering components added to the reorientational contributions.

The physical origin of the persistent negative portion of the AVCF which has emerged from both the DLSS and ISS results and which also shows up in cryogenically cooled CS_2 is not easily understood. It is not clear whether this is a regime of orientational "viscoelasticity"[25] or whether this should be understood in terms of a "*J*" diffusion model as suggested in paper I. Suffice it here to point out the fact that this regime is in fact correlated with the appearance of oscillations in the AVCF and cooling near the freezing point, as demonstrated by the results for CS_2 and methyl iodide at high pressures.[12,25,26]

If, in fact, we are observing the consequences of single-molecule librations, one might rightly ask whether these slight oscillatory correlation components showing up after most of the angular velocity correlation has dissipated are of fundamental importance. We feel that they are, not because of their magnitude but for two main reasons. First, the more structured responses obtained near the freezing point allow a more conclusive differentiation between major dephasing mechanisms of orientational motion in liquids. But just as important are the discrepancies between the appearance of the time-domain scattering data and the correlation functions derived from them and those simulated using MD models of the same liquids near freezing. As stated in the Introduction, to date, MD simulations have not reproduced the qualitative transition to periodic oscillations in derived AVCF's and low-amplitude recurrences in scattering data in the stated thermodynamic regime. Since MD simulation is developing into an elementary tool used to appreciate finer and finer details of liquid-phase molecular phenomena, it is hard to overemphasize the importance of understanding this discrepancy concerning such a fundamental molecular motion. We must question how adequate the potentials used in MD simulations of liquids are for reproducing fine details of dynamical processes in these systems. The selected potentials are usually chosen on the basis of their ability to reproduce thermodynamic averages and may, in principle, be missing essential ingredients for purposes of dynamical simulations. Even MD simulations dedicated specifically to searching for these slight oscillations have been unsuccessful.[37] It is therefore of central importance to test new potentials and to understand why none of the MD simulations to date have reproduced these seemingly fine dynamical details.

VI. Conclusions

We have reported a time-domain light-scattering study of liquid benzene at 280 and 343 K. Analysis of our results using Kubo line-shape theory demonstrates for the first time full quantitative equivalence of the dynamic information obtained from dynamical Rayleigh light scattering and from impulsive stimulated scattering for this system. In light of this, at least in this particular case, the dynamic information extracted could equally be obtained from frequency-domain experiments. In spite of the evidence for II-scattering contributions at early times, we analyze our results in terms of reorientation of single molecules in the liquid and de-

termine that at temperatures below 310 K, we observe evidence of oscillatory AVCF's and that these oscillations become more pronounced as the liquid is cooled further. From the functional form of the extracted AVCF's, we have inferred that inhomogeneity of local structures in the liquid contributes dominantly to the process of librational dephasing. These results join and strengthen a large body of work on numerous molecular liquids, indicating that the transition to oscillatory AVCF's upon cooling is in fact a general phenomenon. Finally, we have discussed the puzzling absence of corroboration for this picture in MD simulations and stressed the importance of investing a renewed effort in understanding this discrepancy.

Acknowledgment. We are indebted to Prof. K. A. Nelson and G. P. Wiederrecht for enlightening discussions and warm hospitality. We thank Dr. E. Mastov for technical assistance. S.R. thanks the Israeli Council for higher education for an Allon Fellowship. This work was supported by the Israel America Binational Science Foundation and the James Franck program for light-induced processes. The Farkas Center is supported by the Bundesministerium fur Forschung and the Minerva Gesellschaft fur die Forschung.

Registry No. Benzene, 71-43-2.

References and Notes

(1) *Statistical Mechanics*; McQuarie, D. A., Ed.; Harper and Row: New York, 1976.
(2) Rothchild, W. G. *Dynamics of molecular liquids*; Wiley: New York, 1984.
(3) Steele, W. A. *Adv. Chem. Phys.* **1976**, *34*, 1.
(4) Gordon, R. G. *J. Chem. Phys.* **1965**, *43*, 1307.
(5) McTague, J. P.; Birnbaum, G. *Phys. Rev. Lett.* **1968**, *21*, 661.
(6) Frenkel, D.; McTague, J. P. *J. Chem. Phys.* **1980**, *72*, 2801.
(7) Madden, P. A.; Tildsley, D. J. *Mol. Phys.* **1985**, *55*, 969.
(8) Madden, P. A.; Tildsley, D. J. *Mol. Phys.* **1983**, *48*, 129.
(9) Kluk, E.; Monkos, K.; Pasterny, K.; Zerda, T. *Acta Phys. Pol. A* **1979**, *56*, 109.
(10) Cox, J. I.; Battaglia, M. R.; Madden, P. A. *Mol. Phys.* **1979**, *38*, 1539.
(11) Bansal, M. L.; Deb, S. K.; Roy, A. P. *Chem. Phys. Lett.* **1981**, *83*, 83.
(12) Dill, J. F.; Litovitz, T. A.; Bucaro, J. A. *J. Chem. Phys.* **1975**, *62*, 3839.
(13) Evans, G. T.; Evans, M. W. *J. Mol. Liq.* **1983**, *25*, 177.
(14) Linse, P.; Engstrom, S.; Jonsson, B. *Chem. Phys. Lett.* **1985**, *115*, 95.
(15) Steinhauser, O. *Chem. Phys. Lett.* **1981**, *82*, 153.
(16) Geiger, L. C.; Ladanyi, B. M. *J. Chem. Phys.* **1987**, *87*, 191. Geiger, L. C.; Ladanyi, B. M. *J. Chem. Phys.* **1988**, *89*, 6588.
(17) Greene, B. I.; Farrow, R. C. *Chem. Phys. Lett.* **1983**, *98*, 273.
(18) Halbout, J. M.; Tang, C. L. *Appl. Phys. Lett.* **1982**, *40*, 765.
(19) (a) Ruhman, S.; Kohler, B.; Joly, A. G.; Nelson, K. A. *IEEE J. Quant. Electron.* **1988**, *24*, 470. (b) Ruhman, S.; Joly, A. G.; Kohler, B.; Williams, L. R.; Nelson, K. A. *Rev. Phys. Appl.* **1987**, *22*, 1717.
(20) McMorrow, D.; Lotshaw, W. T.; Kenney-Wallace, G. A. *Rev. Phys. Appl.* **1987**, *22*, 443. McMorrow, D.; Lotshaw, W. T. *Chem. Phys. Lett.* **1990**, *174*, 85.
(21) Hattori, T.; Terasaki, A.; Kobayashi, T.; Wada, T.; Yamada, A.; Sasaba, H. *J. Chem. Phys.* **1991**, *95*, 937.
(22) Hattori, T.; Kobayashi, T. *J. Chem. Phys.* **1991**, *94*, 3332.
(23) Yan, Y.-X.; Cheng, L. T.; Nelson, K. A. In *Advance in Nonlinear Sepecroscopy*; Clarke, R. G. H., Hester, R. E., Eds.; Wiley: New York, 1987.
(24) Etchepare, J.; Grillon, G. J.; Chambaret, P.; Hamoniaux, G.; Orszag, A. *Opt. Commun.* **1987**, *63*, 329.
(25) Ruhman, S.; Nelson, K. A. *J. Chem. Phys.* **1990**, *94*, 859.
(26) Kohler, B.; Nelson, K. A. *J. Phys. Condens. Matter.* **1990**, *2*, 109.
(27) Etchepare, J.; Grillon, G.; Chambaret, J. P.; Antonetti, A.; Orszag, A. *Rev. Phys. Appl.* **1987**, *22*, 1749.
(28) Dardy, H. D.; Volterra, V.; Litovitz, T. A. *J. Chem. Phys.* **1973**, *59*, 4491.
(29) Yan, Y.-X.; Nelson, K. A. *J. Chem. Phys.* **1987**, *87*, 6240.
(30) Kubo, R. In *Fluctuation, Relaxation and resonance in Magnetic System*; ter Harr, D., Ed.; Oliver and Boyd: Edinburgh, 1992.
(31) Deb, S. K. *Chem. Phys.* **1988**, *120*, 225.
(32) Lynden-Bell, R. M.; Steele, W. A. *J. Phys. Chem.* **1984**, *88*, 6514.
(33) Sizer, T. J.; Kafka, D.; Duling, I. N.; Gabel, C. W.; Mourou, G. A. *IEEE J. Quant. Electron.* **1983**, *19*, 506.
(34) Chesnoi, J.; Fini, L. *Opt. Lett.* **1986**, *11*, 635.
(35) Dawson, M. D.; Maxson, D.; Boggess, T. F.; Smirl, A. L. *Opt. Lett.* **1988**, *13*, 126.
(36) Press, W. H.; Flannery, B. P.; Teukolsky, S. A.; Vettering, W. T. *Numerical Recipes in C*; Cambridge University Press: New York, 1992.
(37) Kohler, B.; Nelson, K. A. *J. Phys. Chem.*, in press.
(38) Hegemann, B.; Jonas, J. *J. Chem. Phys.* **1985**, *82*, 2845.
(39) Geiger, L. C.; Ladanyi, B. M. *Chem. Phys. Lett.* **1989**, *159*, 413.

Mechanism of the Thermally Induced Gas-Phase Decomposition of Silane: A Revisitation

M. A. Ring* and H. E. O'Neal*

Department of Chemistry, San Diego State University, San Diego, California 92182
(Received: February 3, 1992)

Modeling of the SiH_4 thermal decomposition (640–703 K; 80–320 Torr) ia revisited here since new kinetic data now invalidate our prior modeling. The new data are for silylenę insertion reactions, for silylene–disilene isomerizations, and for the H_2 elimination from Si_2H_6. Three possible sink reactions as balance for silylene productions were examined: (1) reactive intermediate polymerization followed by wall deposition, (2) reactive intermediate decomposition to a nonreactive species followed by wall deposition, and (3) direct reaction of polysilanes (Si_3H_8 and larger) on the walls. Using rate constants consistent with all present data, the modeling demonstrated that fits to the experimental data could only be achieved with polysilane-wall decompositions as sink reactions. Rate constants for these wall processes were obtained directly from our published Si_3H_8 decomposition data. In addition, the modeling indicated that best fits to the experimental data were realized with negative activation energies for all silylene Si–H bond insertion reactions in accord with new data on the $SiH_2 + SiH_4$ reaction (Walsh et al.).

Introduction

In 1985 we proposed a mechanism for the silane decomposition under static system conditions: temperatures between 640 and 703 K and total pressures between 80 and 320 Torr.[1] This mechanism, the essential features of which are shown in Scheme I not only explained all of the unusual kinetic behaviors of the silane system but also quantitatively fit the rather demanding product yield observations of Purnell and Walsh[2] (P&W). These were as follows: a $^3/_2$ order in silane initial reaction stage from 0 to 1% silane conversion, a rate accelerated transition stage from 3 to 10% reaction, a first order in silane middle stage from 10 to 30% silane conversion, and a final inhibition stage at conversions above 30%, also $R = (DS)_{max}/(S)_0 = 0.0274 \pm 0.0011$, $R' = (TS)_{max}/(S)_0 = 0.00474 \pm 0.00023$, and $MA = [(DS)^2/(S)\text{-}(TS)]_{max} = 0.20 \pm 0.01$, where S, DS, and TS represent silane, disilane, and trisilane, and subscripts 0 and max refer to the initial and maximum yield conditions, respectively. From the vantage point of nearly a decade of experimental and theoretical inves-

0022-3654/92/2096-10848$03.00/0